

## High-Power Vacuum Window in WR10

Marc E. Hill, Richard S. Callin, and David H. Whittum

**Abstract**—Results are presented in this paper for fabrication and test of a WR10 waveguide window for use in ultrahigh vacuum at 91.4 GHz. Low-power bench measurements are compared with analytic and simulation results. Operation at  $\approx 4$ -kW peak power, duty factor  $10^{-6}$ , and  $10^{-9}$ -scale vacuum is noted.

### I. INTRODUCTION

In a microwave accelerator network, waveguide windows are employed to isolate the  $10^{-7}$ -torr beamline vacuum from the  $10^{-9}$ -torr vacuum of the power tube. The window is essential to long tube life, currently in the range of  $5 \times 10^4$  h for the 65-MW klystrons powering the two-mile accelerator (TMA) [1]. Future accelerators will require shorter wavelengths to reach higher gradients, and research toward a gigavolt per meter linac currently concentrates on *W*-band, at the 32nd harmonic of the 2856-MHz TMA operating frequency [2]. Engineering of such a miniature millimeter-wave linac requires development of a new class of millimeter-wave components, compatible with high vacuum and capable of handling high-peak power, albeit at low duty cycle. Here, we report results of bench and high-power tests of such a window, the first test of such a millimeter-wave assembly in a working accelerator.

### II. FABRICATION AND ASSEMBLY

Conceptually, the window consists of WR10 waveguide, operated in fundamental  $TE_{10}$  mode, and a slab of dielectric filling a length of the guide. Wave transmission through a length  $L$  of lossless dielectric is described by

$$|S_{21}|^2 = \left[ \cos^2 \beta' L + \frac{1}{4} \left( \frac{\beta}{\beta'} + \frac{\beta'}{\beta} \right)^2 \sin^2 \beta' L \right]^{-1} \quad (1)$$

where  $\beta$  and  $\beta'$  are the guide wavenumbers in the vacuum and dielectric portions of the guide

$$\beta = 2\pi\lambda\sqrt{\mu_r\epsilon_r - \left(\frac{\lambda}{2a}\right)^2} \quad (2)$$

$\lambda$  is the free-space wavelength,  $a$  is the waveguide width ( $0.10''$ ), and  $\mu_r$  and  $\epsilon_r$  are the relative permeability and permittivity of the dielectric. For a good match, the window length should be a multiple of half the dielectric guide wavelength, or  $\beta' L = n\pi$ , with  $n$  an integer. In addition, (1) implies that highest bandwidth is attained with the shortest window length. We selected an  $n = 2$  or “ $1 - \lambda$ ” window design as a compromise between bandwidth and ease of assembly.

As to assembly, the  $0.10'' \times 0.050''$  oxygen-free high-conductivity (OFE) copper WR10 rectangular waveguide is obtained unflanged from commercial extruded stock and chemically cleaned. The dielectric consists of WesCo AL-995 alumina ceramic, sliced and ground from a  $3''$  disk, into rods of dimension  $0.098'' \times 0.048'' \times 2''$ . The rods

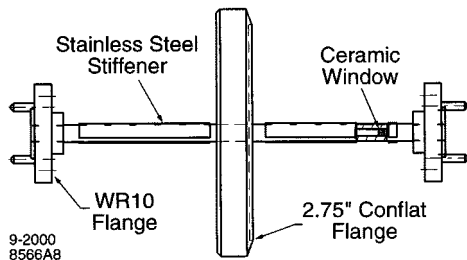


Fig. 1. Mechanical drawing of the final window assembly including RF and vacuum flanges.

are coated with a 1-mil layer of molybdenum–manganese and fired at  $1500^\circ\text{C}$ , forming a metallized layer for brazing. The windows are then cut to their final length of  $0.0428''$  and brazed into the OFE waveguide. The waveguide flanges are attached in a separate step. They consist of 304L vacuum-arc remelt (VAR) stainless steel, machined to the standard  $3/4''$  circular WR10 waveguide flange geometry. These are attached with a second lower temperature braze. After each braze step, the window is leak checked to ensure vacuum integrity.

One concern with this process is the difference in the thermal expansion coefficient of the ceramic ( $9.3 \times 10^{-6}/^\circ\text{C}$ ) and the copper waveguide ( $17 \times 10^{-6}/^\circ\text{C}$ ). Differential expansion during the  $1000^\circ$  braze cycle may, in principle, produce a gap as large as 1 mil between the dielectric and copper surfaces. For lower frequency larger dimension window assemblies, such differential expansion may be restrained by a molybdenum retaining wire encircling the ceramic window assembly. We omitted this step for the *W*-band assembly, and encountered no problems, although one might expect that its use would produce a smaller braze fillet.

### III. MEASUREMENTS

The completed window assembly seen in Fig. 1 was subjected to transmission and reflection measurements in WR10 using a custom-built vector network analyzer described in [3]. The results, seen in Fig. 2, were fit with the analytic result of (1), employing  $\epsilon_r$  as a fit parameter. We infer  $\epsilon_r \approx 9.485 \pm 0.03$  at 91.4 GHz. Also seen in Fig. 2 is the result of numerical simulation via the finite-difference code *GdfidL* [4], giving good agreement.

One additional concern in this geometry is the presence of higher modes, i.e., “ghost modes,” in the overmoded dielectric guide. One is particularly concerned to avoid a spurious resonance in the operating band and the added insertion loss that would result. Fig. 2 shows the power sum  $|S_{11}|^2 + |S_{21}|^2$ , from which we can determine the insertion loss, and inspect the operating band for ghost modes. The observed attenuation of 0.2 dB seen in Fig. 2 is consistent with loss through the  $3''$  copper waveguide. With such a short length of ceramic, results are not sensitive to a loss tangent in the  $10^{-4}$  range.

After bench measurements, this window was employed on the output of a test cavity installed on a microwave accelerator at the Stanford Linear Accelerator Center (SLAC), Stanford University, Stanford, CA. This experiment, to be described in a later paper, produced peak power levels of 4 kW. This corresponds to a maximum electric field in the waveguide of 1.5 MV/m. The window was an essential component for this test as the solid-state components needed for power detection are not vacuum compatible, and, in any case, are most conveniently situated outside the vacuum envelope.

The design and process appear to be mechanically sound and robust; following the first working window, several additional windows have been fabricated, and their RF characteristics are in close agreement

Manuscript received July 25, 1999. This work was supported by the U.S. Department of Energy under Contract DE-AC03-76SF00515.

M. E. Hill is with the Physics Department, Harvard University, Cambridge, MA 02138 USA.

R. S. Callin and D. H. Whittum are with the Stanford Linear Accelerator Center, Stanford University, Stanford, CA 94309 USA.

Publisher Item Identifier S 0018-9480(01)03323-3.

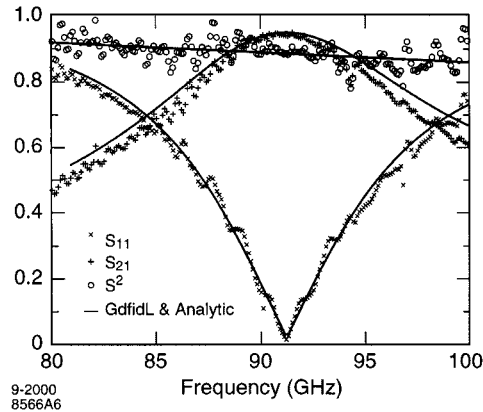


Fig. 2. Plot of measured scattering parameters  $S_{11}$  and calculated scattering parameters for a sample window ( $S^2 = S_{11}^2 + S_{21}^2$ ).

with the foregoing, while they have all passed a leak check. Thus far, we have seen no evidence of breakdown, multipactor, fracture, or puncture, even while realizing that such phenomena are part of the experiment, and part of the utility of the apparatus in the first place.

#### IV. CONCLUSIONS

We have begun to develop vacuum-compatible components in WR10 for operation with a miniature accelerator. The immediate and initial purpose for the window was to permit monitoring of power developed in a subharmonic interaction circuit. Alternatives to a window include coaxial feedthrough, horn output through a window, taper to oversize guide, and window. However, all of these techniques have their own challenges and, even if successful, leave one with a more complicated power calibration. More than that, they are not ideally suited for accelerator component development. With a WR10 window, we can couple power to other WR10 components in a straightforward way. We expect that development of more sophisticated quasi-optical accelerator components will later benefit from the calibrations and other work facilitated by this simple, yet robust, window design.

#### ACKNOWLEDGMENT

The authors wish to acknowledge the support and encouragement of G. Caryotakis, Stanford Linear Accelerator Center (SLAC), Stanford University, Stanford, CA, and J. Huth, Harvard University, Cambridge, MA, helpful conversations with W. R. Fowkes, SLAC, Stanford University, Stanford, CA, and the expert assistance of D. Miller, SLAC, Stanford University, Stanford, CA, and D. Millican, SLAC, Stanford University, Stanford, CA.

#### REFERENCES

- [1] G. Caryotakis, "High power microwave tubes: In the laboratory and on-line," *IEEE Trans. Plasma Sci.*, vol. 22, pp. 683-691, Oct. 1994.
- [2] D. H. Whittum, "Ultimate gradient in solid-state accelerators," in *Proc. Adv. Accelerator Concepts Workshop*.
- [3] R. H. Siemann. W-band vector network analyzer based on an audio lock-in amplifier. *Phys. Rev.*, unpublished.
- [4] W. Bruns, "GdfidL: A finite difference program for arbitrarily small perturbations in rectangular geometries," *IEEE Trans. Magn.*, vol. 32, pp. 1453-1456, May 1996.

## A Technique for Determining the Normalized Impedance of Slots in the Image Plane of the Image NRDG

Lawrence C. Chirwa, Manabu Yamamoto, Manabu Omiya, and Kiyohiko Itoh

**Abstract**—This paper presents a method for determining the normalized impedance of a transverse slot in the image plane of the image nonradiative dielectric guide using measurements of the standing wave. The method overcomes the problem of distortion caused by the scattered evanescent fields that are present in the vicinity of the slot. The measurement equipment, its optimum parameters, and aspects necessary for accurate measurements are also discussed. Moreover, the finite-difference time-domain technique is employed to determine the normalized slot impedance, and good agreement is obtained with measured results, confirming the reliability of the method.

**Index Terms**—FDTD technique, image NRD guide, measurement of standing wave, millimeter-wave, normalized impedance, slot in the image plain.

#### I. INTRODUCTION

Low insertion loss is one of the important properties that millimeter waveguides should have. The nonradiative dielectric waveguide (NRDG) [1] is one of the waveguides that posses this characteristic. The image nonradiative dielectric waveguide (iNRDG) [2], [3] is derived from the normal NRDG, and it has low insertion loss, very much like that of the normal NRDG from which it is derived. However, it has the advantage over the normal NRDG of being smaller in size.

The principle operation mode of the iNRDG is the lowest LSM mode, the  $LSM_{10}$  mode. As the  $LSM_{10}$  mode of the iNRDG is similar to the  $TE_{10}$  mode for rectangular waveguides, the design method for waveguide slot array antennas proposed in [4] and [5] can be used to design an iNRDG slot array antenna consisting of transverse slot elements. In order to utilize this design method, the normalized impedance of the transverse slot in the image plane needs to be known.

In this paper, we propose a method for determining the normalized impedance of a transverse slot that utilizes experimental measurements of the standing wave in the waveguide and takes into consideration the distortion effects of the higher mode evanescent fields in the vicinity of the slot. The equipment for measuring the standing wave and the optimum parameters of the probe used to measure the standing wave are also described. The normalized impedance results obtained using the technique proposed in this paper are validated by comparing them to results obtained using finite-difference time-domain (FDTD) analysis [6].

#### II. MEASUREMENT OF THE STANDING WAVE

The necessity of taking precise measurements of the fields of the standing-wave profile in order to accurately estimate the normalized impedance of the slot cannot be over emphasized. From the relationships used to determine the reflection coefficient, it is apparent that it is especially important to make precise measurements of the standing wave when the standing wave ratio (SWR) is almost equal to one. In this

Manuscript received July 16, 1999; revised March 2, 2000. This work was supported by the Ministry of Education, Science, Sports, and Culture of Japan under Grant-in-Aid for Developmental Scientific Research (A) (2) 11355017.

The authors are with the Graduate School of Engineering, Hokkaido University, Sapporo 060-8628, Japan.

Publisher Item Identifier S 0018-9480(01)03311-7.